par-6, a gene involved in the establishment of asymmetry in early *C. elegans* embryos, mediates the asymmetric localization of PAR-3

Jennifer L. Watts[1], Bijan Etemad-Moghadam[1], Su Guo[1], Lynn Boyd[1], Bruce W. Draper[2], Craig C. Mello[2,*], James R. Priess[2] and Kenneth J. Kemphues[†]

[1]Section of Genetics and Development, Cornell University, Ithaca, New York 14853, USA
[2]Howard Hughes Medical Institute, Department of Basic Sciences, Fred Hutchinson Cancer Research Center, 1124 Columbia St, Seattle, Washington 98109, USA

*Present address: University of Massachusetts Cancer Center, 2 Biotech, Suite 202, 373 Plantation Street, Worcester, MA 01605, USA
†Author for correspondence (e-mail: kjk1@cornell.edu)

SUMMARY

The generation of asymmetry in the one-cell embryo of *Caenorhabditis elegans* is necessary to establish the anterior-posterior axis and to ensure the proper identity of early blastomeres. Maternal-effect lethal mutations with a partitioning defective phenotype (*par*) have identified several genes involved in this process. We have identified a new gene, *par-6*, which acts in conjunction with other *par* genes to properly localize cytoplasmic components in the early embryo. The early phenotypes of *par-6* embryos include the generation of equal-sized blastomeres, improper localization of P granules and SKN-1 protein, and abnormal second division cleavage patterns. Overall,

this phenotype is very similar to that caused by mutations in a previously described gene, *par-3*. The probable basis for this similarity is revealed by our genetic and immunolocalization results; *par-6* acts through *par-3* by localizing or maintaining the PAR-3 protein at the cell periphery. In addition, we find that loss-of-function *par-6* mutations act as dominant bypass suppressors of loss-of-function mutations in *par-2*.

Key words: embryogenesis, cell polarity, suppression, *Caenorhabditis elegans*, axis, *par-6*, assymmetry

INTRODUCTION

A dramatic reorganization of cytoplasm occurs in the *C. elegans* egg after fertilization (Nigon et al., 1960). During this reorganization, the anterior and posterior poles of the egg display several different characteristics. Foci of filamentous actin accumulate transiently at the anterior pole, and anterior contractions result in an incomplete cleavage called a psuedocleavage. Cytoplasm associated with the outermost cortex of the egg flows toward the anterior pole, and non-cortical cytoplasm streams toward the posterior pole (Hird and White, 1993). Cytoplasmic P granules, which later associate with the germline cells, become localized to the posterior pole (Strome and Wood, 1982, 1983). The maternal and paternal pronuclei join in the posterior and migrate to the center of the cell. The first mitotic spindle becomes asymmetrically positioned in the cell and the first division is unequal (Albertson, 1984; Kemphues et al., 1988b).

After division, the anterior daughter, called AB, differs markedly from the posterior daughter, P1 (Sulston et al., 1983). For example, only AB expresses GLP-1, a membrane receptor that is required for anterior cell fates in the early embryo, and only P1 contains P granules. SKN-1, a transcription factor that specifies the fate of ventral blastomeres in the early embryo, is much more abundant in the P1 nucleus than in the AB nucleus (Bowerman et al., 1993). AB and P1 also have different cell-

cycle periods and cleavage patterns; at cleavage the AB spindle is transverse, and the P1 spindle is longitudinal, with respect to the long axis of the egg.

To determine the genetic basis for anterior/posterior differences in the *C. elegans* embryo, mutants have been isolated in which these differences are reduced or absent (Kemphues, 1989; Kemphues et al., 1988b). Mutations in five *par* genes (partitioning defective) can result in embryos in which AB and P1 have equal distributions of P granules, equal cell cycles, and similar spindle alignments (Kemphues, 1989; Kemphues et al., 1988b). Many of the early phenotypes of *par* mutants, such as improper P granule localization, equal division of the fertilized zygote, and incorrect spindle alignments in AB and P1 can be phenocopied by a brief pulse of cytochalasin D during a critical period of the first cell cycle (Hill and Strome, 1990), indicating that the *par* gene products could be regulating microfilaments or interacting with them.

Three of the *par* genes have been cloned and the intracellular distributions of their protein products have been determined. *par-1* encodes a putative serine/threonine kinase that is localized to the posterior cortex of the one-cell embryo, and continues to be asymmetrically distributed in the P lineage during subsequent divisions (Guo and Kemphues, 1995). The *par-2* gene encodes a novel protein with a myosin-like ATP binding site and a conserved cysteine-rich domain (Levitan et al., 1994) and has a localization pattern

similar to PAR-1 (see accompanying paper by Boyd et al., 1996). The *par-3* gene encodes a novel protein that is localized to the anterior periphery of the one-cell embryo; a distribution that is the reciprocal of PAR-1 and PAR-2 (Etemad-Moghadam et al., 1995). In subsequent stages PAR-3 is present uniformly at the periphery of somatic cells but in the germ line lineage it maintains its reciprocal relationship with PAR-1 and PAR-2.

In this paper we describe the characterization of *par-6*, a new gene involved in the generation of asymmetry in the early embryo. We show that mutations in *par-6* result in the disruption of many asymmetries, including P granule localization, SKN-1 localization, and spindle orientations at the second division. We show that *par-6* mutations act as dominant bypass suppressors of *par-2* mutations, and can enhance weak *par-3* mutations. Finally, in *par-6* mutants the PAR-1, PAR-2, and PAR-3 proteins are improperly localized in early embryos. We propose that the *par-6* gene product is necessary to localize or maintain PAR-3 protein at the periphery of early embryos.

MATERIALS AND METHODS

Strains and maintenance

C. elegans strains were maintained as described by Brenner (1974). The genetic markers, deficiencies, and balancer chromosomes used are listed by linkage group (LG) as follows: LGI, *dpy-5(e61)*, *unc-101(m1)*, *unc-13(e1091)*, *lin-11(n386)*, *unc-75(e950)*, *par-6(zu170)*, *par-6(zu174)*, *par-6(zu222)*, *hT2(I'; III)*, *hIn1 unc-54*, *hDf15(h1486)*, *hDf16(h1487)*, *hDf17(h1488)*; LGII, *bli-2(e768)*; LGIII, *par-2(it5ts)*, *par-2(lw32)*, *daf-5(e1372ts)*, *par-3(e2074)*, *par-3(it71)*, *lon-1(e185)*, *qC1*, *dpy-1(e1)*, *sC1*; LGIV, *unc-5(e53)*; LGV, *dpy-11(e224)*; X, *lon-2(e678)*. Most mutations are described by Wood (1988). The LGI balancers *hT2 (I; III)*,*hIn1 unc-54* are described by Edgley et al. (1995). The deficiencies *hDf15*, *hDf16*, and *hDf17* were gifts from Fred Ho and Ann Rose and the deficiency *sy216* was a gift from Paul Sternberg (Lee et al., 1994). The term 'par-6 embryos' refers to embryos produced by homozygous *par-6* mothers.

All strains were grown at 20°C except for temperature-sensitive alleles, which were maintained at 15°C, the permissive temperature, and shifted to the restrictive temperature, 25°C, for analysis of the mutant phenotypes.

Mapping and complementation

The *par-6* mutations were mapped to LGI by standard linkage tests. Two- and three-factor crosses showed that *par-6* maps between *unc-101* and *glp-4*, 0.7 map units to the right of *unc-101*. Mapping data are available from the Caenorhabditis Genetics Center, University of Minnesota.

For complementation tests with *hDf15*, *hDf16*, *hDf17* and *sy216*, deficiencies that delete *unc-101*, hermaphrodites of the genotype *Df/hIn1* were crossed to *par-6 unc-101/hIn1* males. F₁ Unc-101 progeny were picked individually and tested for maternal effect lethality. *hDf15*, *hDf16*, and *sy216* were found to delete the *par-6* locus.

Observing early development in live embryos

Embryos were dissected out of gravid hermaphrodites in water and transferred to a polylysine coated slide (Kirby et al., 1990), mounted under a coverslip supported by enough petroleum jelly to preclude contact with the embryos. The embryos were examined with Nomarski optics under a Zeiss microscope equipped with a video camera, and the period from pronuclear migration to the four-cell

stage was videorecorded. Spindle orientations were scored as described by Cheng et al. (1995).

Indirect immunofluorescence

P granules were visualized with OIC1D4 antibodies (gift from S. Strome) according to the procedure of Strome and Wood (1983). Spindles were visualized using a monoclonal antibody against *Drosophila* alpha-tubulin (gift from M. Fuller, Stanford University) according to procedures previously described (Albertson, 1984; Kemphues et al., 1986). Staining with the monoclonal antibody FA2 against SKN-1 protein followed the procedures of Bowerman et al. (1993). Immunofluorescence assays for terminal differentiation markers followed the method of Kemphues et al. (1988), using the monoclonal antibodies 5.6 (body wall myosin; Miller et al., 1983), 9.2.1 (pharyngeal myosin; Epstein et al., 1982), and MH27 (adherens junctions; Francis and Waterston, 1985). Staining with anti-PAR-1 antibodies was performed as described by Guo and Kemphues (1995), PAR-2 staining followed Method II from Waddle et al. (1994) as described by Boyd et al. (1996), and PAR-3 staining was performed as described by Etemad-Moghadam et al. (1995).

Western blot analysis

Approximately 300 gravid wild-type and homozygous *unc-13 par-6(zu222)* hermaphrodites were hand picked and washed with M9 buffer. Embryo isolation and western blot preparation followed the method of Etemad-Moghadam et al. (1995). The blot was probed with purified anti-PAR-3 antibody or monoclonal anti-tubulin and horseradish peroxidase-linked anti-rabbit IgG (anti-mouse for tubulin) and detected using the ECL system (Amersham).

Construction of *par-2*; *par-6*, *par-2*; *par-6/+* and *par-2*; *hDf15/+*

daf-7 par-2 (it5ts) III hermaphrodites were mated with *unc-13 par-6/hT2 (I; III) dpy-5* males at 15°C. Cross progeny were mated to their F₁ siblings and the F₂ progeny were grown at 25°C. F₂ Dafs were picked individually to 15°C to recover *daf-7 par-2* homozygotes. Worms that segregated both Dpy and Unc progeny were presumed to be *daf-7 par-2; unc-13 par-6/hT2 dpy-5. (I); daf-7 par-2 (III)*. (The *hT2 dpy 5(I); daf-7 par-2 (III)* translocation is abbreviated as *hT2 par-2* below). Unc progeny were picked individually to 15°C to confirm the presence of *par-6*. The Dafs (*daf-7 par-2; unc-13 par-6/hT2, par-2*) and Dpy Dafs (*daf-7 par-2; hT2 par-2*) were picked individually to 25°C and scored for maternal-effect lethality (Mel) to confirm the presence of *par-2*. The Dpy Dafs were Mel, indicating that the strain was homozyous for *par-2*, but due to the suppression described in the Results section, the non-Dpy Dafs (*daf-7 par-2; par-6/hT2 par-2*) produced a large number of hatching embryos. The *par-2; par-6* double homozygotes were identified as Daf Unc animals.

To better quantify the extent of suppression without the lethality caused by heterozygosity for the balancer *hT2*, worms of genotype *daf-7 par-2 (it5ts); unc-101 par-6 (zu170)/+* were constructed. We crossed *daf-7 par-2 (it5ts)* hermaphrodites to *unc-101 par-6/hIn1* males at 15°C. F₁ cross progeny were allowed to self at 25°C and F₂ Dafs were plated individually at 25°C. Daf nonUncs that recovered from dauer were scored for Mel. Two classes were identified, as expected. One class had low viability (*daf-7 par-2; +/+*); a second class had 70-90% viable embryos and segregated Unc progeny (*daf-7 par-2; +/unc-101 par-6*).

Non-balanced strains were also constructed using the other *par-6* alleles *zu174* and *zu222*. However, these strains were not marked with *unc-101*. In these two constructs, we inferred the genotype based on the suppression of *par-2*. This was possible because the progeny of *daf-7 par-2; par-6/+* always gave a bimodal distribution, with half the worms giving greater than 48% viable embryos (*daf-7 par-2; par-6/+*) and the other half giving less than 24% viable embryos, the highest value seen among control *daf-7 par-2* homozygotes (*daf-7 par-2; par-6/par-6* or *+/+*).

Worms of genotype *dpy-1 par-2(lw32); par-6/+* were constructed in a similar manner as described above.

To construct *dpy-1 par-2(lw32); hDf15/+* worms, *dpy-1par-2(lw32)/sC1* hermaphrodites were mated to *hDf15/hIn1* males. Cross progeny were plated individually and Dpy progeny of *dpy-1 par-2/+; hDf15/+* mothers were picked individually. Many Dpy worms gave survival rates higher than 16%, the highest control value for *dpy-1 par-2(lw32)*, indicating suppression of *par-2 (lw32)* by *hDf15*. However, these worms did not give the same bimodal distribution seen with *zu170* and *zu222*. The worms showed a continuous range of survival from 1-63%, making it impossible to deduce the genotype of each worm. To obtain the data in Table 2 only those worms with greater than 18% viable progeny were included. The number of total progeny from *dpy-1 par-2(lw32); hDf15/+* mothers in Table 2 was adjusted for the lethality of *hDf15* homozygotes.

Construction of *par-3; par-6* double mutants

lon-1par-3(e2074)/qC1 hermaphrodites were mated to *unc-101 par-6(zu170)/hIn1* males. Cross progeny were mated to each other and the progeny of this $F_1 \times F_1$ cross were plated individually and screened for the presence of all markers. A strain of the genotype *unc-101 par-6(zu170)/hIn1; lon-1 par-3(e2074)/++* was obtained and double homozygotes were recognized as Lon Unc animals.

RESULTS

Identification and genetic characterization of *par-6*

During a screen for maternal effect lethal mutations in a mutator strain (Mello et al., 1994), we recovered several mutations that exhibited equal first cleavage and synchronous second cleavages with longitudinal spindle orientations in both blastomeres. Because this phenotype resembled that of *par-3* mutants (Cheng et al., 1995; Kemphues et al., 1988b), we carried out complementation tests with *par-3* mutations. Three mutations (*zu170*, *zu174*, and *zu222*) complemented *par-3* and mapped to linkage group I, 0.7 map units to the right of *unc-101*. The mutations fail to complement the deletions *hDf15*, *hDf16* and *sy216*, placing them in a region devoid of other known mutations (A. Rose, personal communication). Thus, the mutations define a new gene that we call *par-6*.

Each of the *par-6* mutations causes a strict maternal effect, with no evidence of zygotic or paternal effects. Hermaphrodites of the genotype *unc-101 par-6(zu170)/++* produce viable self-progeny at a frequency of 98.5% (*n*=1,398), similar to *unc-101/+* hermaphrodites (99%, *n*=1,056), indicating that *par-6 (zu170)* is recessive and that homozygous *par-6(zu170)* embryos are viable when the mother is heterozygous. Less than 1% of embryos produced by hermaphrodites homozygous for *unc-13 par-6* hatched (1/7241 for *zu222*, 0/5115 for *zu222/hDf15*, 1/8465 for *zu174*, 4/11,694 for *zu170*), and these escapers arrested in larval stages or became agametic adults. To determine if the maternal effect lethality is rescuable by wild-type male sperm, we crossed *plg-1; him-5* males to *par-6(zu222)/hDf15* hermaphrodites. Mated hermaphrodites were scored for the presence of a vulval plug (Kemphues et al., 1988a) and none of the embryos laid by these animals hatched (>400). Expression of *par-6(+)* is not required for male fertility since *dpy-5 unc-101* hermaphrodites produced viable cross progeny when mated to males of the genotype *unc-13 par-6(zu222)/hDf15*.
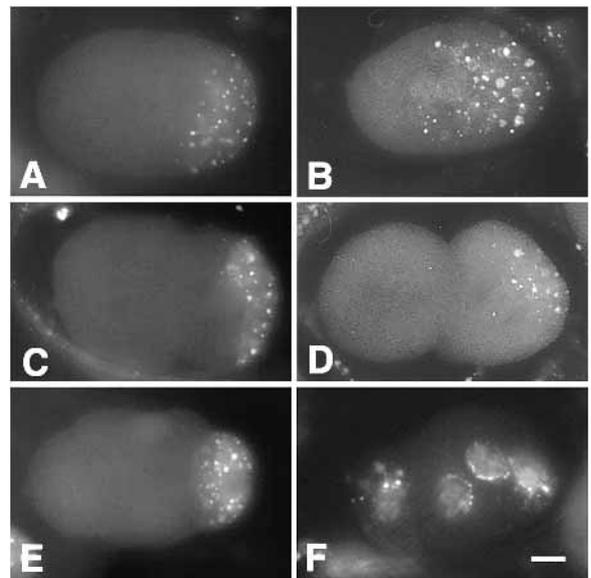

Fig. 1. P granule distribution in wild-type and *par-6* embryos. The P granule distribution is variable in *par-6* embryos; these embryos represent the phenotype observed most frequently during these stages of early embryogenesis. Posterior is to the right. The left column shows wild-type embyos (A,C,E), and the right column shows *par-6(zu222)* mutant embryos (B,D,F) at comparable stages of development; meeting of the pronuclei at the one-cell stage (A,B), two-cell stage (C,D), and the four-cell stage (E,F). In wild-type embryos P granules are localized to the posterior half of the one-cell embryo (A), the P1 blastomere of the two-cell embryo (C) and the P2 blastomere of the four-cell embryo (E). In *par-6* mutants, at the time of pronuclear meeting, 83% of embryos showed significant numbers of P granules in the anterior half of the embryo (*n*=18) (B). By the time the embryo enters metaphase of mitosis, 76% of embryos display P granule staining only in the posterior (*n*=21). In two-cell *par-6* embryos, 93% of embryos showed P granules only in the posterior blastomere (*n*=40) (D). In four-cell *par-6* embryos, 54% of embryos had staining in all four blastomeres (F), 42% had P granules evenly distributed between the two posterior blastomeres, and 3% had P granules present only in the most posterior blastomere. Bar, 10 μm.

Each of the *par-6* mutations cause similar embryonic phenotypes. All *par-6* embryos arrest as amorphous masses of differentiated cells. 98% of late stage embryos are positive for staining with monoclonal antibodies which specifically stain body wall myosin or pharyngeal myosin. 98% also show staining with monoclonal antibody MH27, which stains the adherens junctions of the hypodermal and intestinal cells. Staining is present both internally and on the embryo surface, consistent with the presence of both intestine and hypodermal cells. To assess the presence of intestinal cells, we scored for birefringent gut granules under polarized light (Laufer et al., 1980). *par-6* embryos are variable in their production of gut granules; 51% to 70% of embryos produce gut granules, depending on the allele examined (Table 1). This seems to be a sensitive marker for the severity of the alleles, and suggests that *par-6(zu222)* is the strongest allele. Furthermore, since both *par-6(zu222)/hDf15* and *par-6(zu170)/hDf15* embryos produce intestine slightly less frequently than embryos of *par-6(zu222)* or *par-6(zu170)* homozygotes (Table 1), it is possible that these are not complete loss-of-function
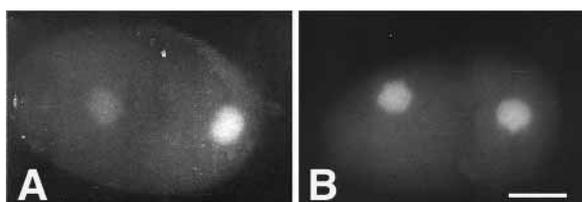
Fig. 2. SKN-1 distribution in wild-type (A) and *par-6(zu222)* (B) two-cell embryos. Posterior is to the right. Bar, 10 μm.

mutations. We conclude that *par-6*, like the other *par* mutants, produce differentiated cell types but in abnormal numbers and patterns.

Early markers of polarity are improperly distributed in *par-6* embryos

In *par-6* embryos, several aspects of P-granule localization are abnormal, although some polarity remains. Fig. 1 depicts the most common P-granule staining patterns observed in the one-, two-, and four-cell wild-type and *par-6* mutant embryos. In the wild-type one-cell embryo, P granules become localized posteriorly during pseudocleavage as the pronuclei condense and migrate toward each other, such that by the time the pronuclei have met, virtually all embryos show complete posterior P-granule localization (Fig. 1A) (Rose et al., 1995; Strome and Wood, 1983). In many *par-6* mutant embryos, P granules remain in the anterior half of the embryo until late in the one-cell stage (Fig. 1B). By the time the one-cell embryo enters metaphase of mitosis, however, most *par-6* embryos display P-granule staining only in the posterior (see Fig. 1 legend). At the two-cell stage, most *par-6* embryos showed P granules only in the posterior blastomere (Fig. 1D), yet, surprisingly, four-cell embryos often displayed P granules in all four blastomeres (see Fig. 1 legend, and Fig. 1F). In late stage embryos (>50 cells), no P granule staining is detectable.

The *skn-1* gene encodes a putative transcription factor that is required for the fate of the EMS blastomere (Bowerman et al., 1992). In wild-type two-cell embryos, SKN-1 protein is present in the nuclei of both blastomeres; however, it is more abundant in the nucleus of the P1 blastomere than in the nucleus of AB (Fig. 2A) (Bowerman et al., 1993). In four-cell embryos it is more abundant in EMS and P2 nuclei than in the nuclei of the AB daughters. We examined early *par-6(zu222)* embryos stained with SKN-1 antibody F2A and found that

Table 1. Intestinal differentiation* in *par-6* embryos

Genotype	% with gut granules	*n*
par-6(zu170) unc-13	70	267
par-6(zu174) unc-13	66	241
par-6(zu222) unc-13	51	227
par-6(zu170)/hDf15	60	361
par-6(zu174)/hDf15	46	330
par-6(zu222)/hDf15	47	208
hDf15/hIn1	100	149
par-6(zu170) unc101; par-3(e2074) lon-1	9	253
par-6(zu170) unc101; par-3(e2074) lon-1/++	67	206
par-6(zu170) unc101/++; par-3(e2074) lon-1	57	248

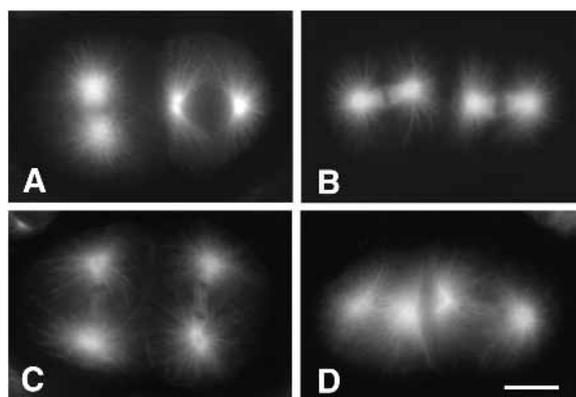*Differentiation is scored by the presence of gut granules in terminal stage embryos.

Fig. 3. Spindle orientation in two-cell wild-type and mutant embryos as revealed by immunofluorescence visualization of tubulin. (A) wild-type embryo (AB in anaphase, P1 in metaphase), (B) *par-6 (zu222)* embryo (metaphase); >90% of embryos (*n*>30 for each of the three alleles) display longitudinal cleavage orientation in both blastomeres, (C) *par-2 (lw32)* embryo (anaphase), and (D) *par-2 (lw32); par-6 (zu222)* double mutant embryo (anaphase). Bar, 10 μm.

SKN-1 protein was present in equal amounts in both nuclei of about half of the two-cell embryos examined (56%, *n*=9) (Fig. 2B) or in all four nuclei in over half of four-cell embryos examined (65%, *n*=17).

Mutations in *par-6* and *par-3* cause similar defects in early cleavage patterns

At the first division of the *C. elegans* embryo, the mitotic spindle is aligned parallel to the long axis of the egg. In wild-type embryos, this spindle is positioned asymmetrically such that the AB daughter is larger than the P1 daughter. In *par-6* embryos, like most *par* mutants (Kemphues et al., 1988b), the first mitotic spindle is located in the center of the fertilized egg, and the AB and P1 daughters have similar sizes.

At the second cleavage of a wild-type embryo, the AB and P1 blastomeres have different centrosome morphologies and have distinct mitotic spindle orientations. The AB centrosome is spherical, with an axial ratio (the ratio of the transverse axis to the longitudinal axis of the centrosome) of about 1.2. The P1 centrosome is disc-shaped, with an axial ratio of about 4.4. We find that AB and P1 centrosomes in *par-6* mutant embryos are both disc-shaped with axial ratios of 2.6 and 2.8, respectively (*n*=7). In wild-type mitosis, the AB spindle becomes aligned transversely with respect to the first division axis. In P1, however, the centrosomal-nuclear complex undergoes a rotation such that the spindle aligns longitudinally, or parallel to the first division axis (Fig. 3A) (Hyman and White, 1987). In *par-6* embryos, the centrosomal-nuclear complex rotates in both AB and P1, such that both blastomeres have longitudinal spindles (Fig. 3B)

Two general classes of *par* mutations have been distinguished previously by their effects on the centrosome morphology and spindle alignment in the AB and P1 blastomeres. In most *par-2* and *par-5* mutant embryos, and in about 20% of *par-1* and *par-4* mutants, both the AB and P1 spindles align transversely (Kemphues et al., 1988b; Morton et al., 1992). In *par-3* mutants, both AB and P1 have disc-shaped centrosomes with axial ratios of about 2.2, and both the spindles of AB and

P1 align longitudinally (Cheng et al., 1995). Thus *par-6* mutants closely resemble *par-3* mutants in centrosome morphology and spindle alignment.

Mutations in *par-6* and *par-3* cause similar mislocalization of PAR-1 and PAR-2 proteins

In wild-type embryos, both PAR-1 and PAR-2 proteins are localized to the posterior periphery of the one-cell embryo (Guo and Kemphues, 1995; Boyd et al., 1996). This asymmetric distribution depends upon *par-3* activity; in one-cell embryos from *par-3* mutants, both of these proteins are still peripherally localized but their distribution is uniform and the peripheral signal is weaker than in wild type (Etemad-Moghadam et al., 1995; Boyd et al., 1996). To determine whether *par-6* function was also required, we examined PAR-1 and PAR-2 distributions in *par-6* embryos. In more than 20 embryos examined for each, the distributions of PAR-1 and PAR-2 are similar to those seen in *par-3* mutants. (Fig. 4).

PAR-3 protein is not properly localized in *par-6* mutants

The striking similarity in the phenotypes of *par-6* and *par-3* mutants raised the possibility that the two genes might act independently in the same process, or that one gene might regulate the expression of the other. To investigate the second possibility, we examined the expression pattern of PAR-3 protein in *par-6* mutant embryos. We first tested if PAR-3 protein was present in *par-6* mutants by western blot analysis of embryonic proteins, and found that *par-6* mutants had wild-type levels of PAR-3 (Fig. 5).

In wild-type embryos the PAR-3 protein has a complex and dynamic distribution (Etemad-Moghadam et al., 1995). Briefly, PAR-3 is localized to the anterior periphery of a one-cell embryo; after the first division, PAR-3 surrounds the AB blastomere, but is present only at the anterior periphery of P1. This pattern of expression is reciprocal to that of the PAR-1 and PAR-2 proteins, which are present at the posterior periphery of P1 (Guo and Kemphues, 1995; Boyd et al., 1996).

We stained *par-6* embryos with antibodies that recognize PAR-3, and found similar abnormalities in PAR-3 localization in each of the strains tested (*par-6(zu170)*, *par-6(zu222)*, and
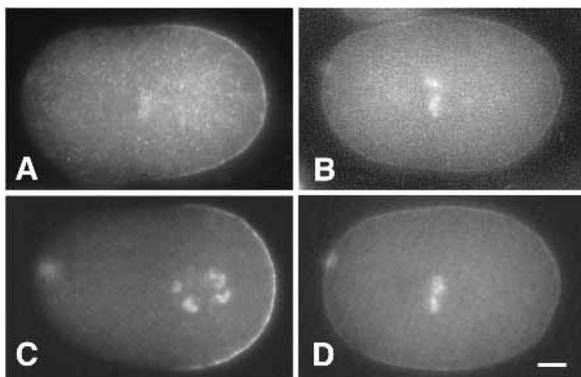

Fig. 5. Western blot of wild-type (N2) and *par-6(zu222)* embryo extracts probed with anti-PAR-3 antibody and with anti-tubulin antibody as a loading control.

par-6(zu222)/hDf15). In *par-6* mutants PAR-3 peripheral staining is reduced or absent (Fig. 6). In addition, when staining is detectable, it is not always asymmetric. Because *par-6* mutants appear to have wild-type levels of PAR-3 protein, we conclude that the wild-type pattern of PAR-3 localization requires *par-6(+)* activity.
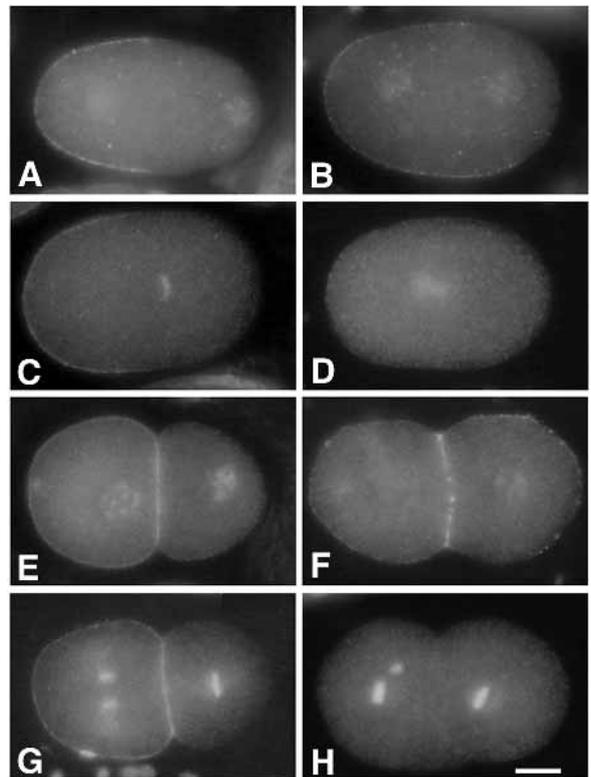
Fig. 6. PAR-3 staining in wild-type and *par-6(zu222)* embryos. Posterior is to the right. The left column shows wild-type embyos (A,C,E,G), and the right column shows *par-6(zu222)* mutant embryos (B,D,F,H) at comparable stages of development. 66% of pronuclear stage *par-6* embryos showed faint, asymmetric staining (B), 11% showed faint, symmetric staining and the remaining 23% showed no detectable staining (*n*=38). 68% of late one cell stage *par-6* embryos showed no detectable staining (D), 22% showed faint, asymmetric staining and 11% showed faint, symmetric staining (*n*=31). 89% of interphase two-cell *par-6* embryos showed faint, symmetrical staining (F), while 11% showed no staining (*n*=28). 38% of two-cell metaphase *par-6* embryos showed no detectable staining (H), while 58% showed faint, symmetric staining, and 4% showed faint, asymmetric staining (*n*=26). Bar, 10 μm.

Fig. 4. PAR-1 and PAR-2 staining in wild-type and *par-6* embryos. Posterior is to the right. The left column shows wild-type one-cell embryos stained with PAR-1 (A) and PAR-2 (C). The right column shows *par-6(zu222)* one-cell embryos stained with PAR-1 (B) and PAR-2 (D). Bar, ~10 μm.
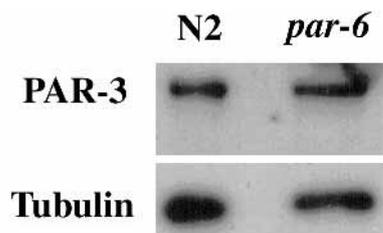
Table 2. Suppression of *par-2* maternal-effect lethality and maternal-effect sterility by *par-6*

Genotype	No. hatched/No. eggs laid	No. fertile progeny/total progeny
daf-7 par-2(it5ts) (25°C)	60/799 (8%)	8/36 (22%)**
unc-13 par-6(zu170)	1/1649 (<1%)	0
unc-13 par-6(zu222)	1/1056 (<1%)	0
daf-7 par-2(it5ts); unc-101 par-6 (zu170)/+	1691/1979 (85%)	35/38 (92%)**
daf-7 par-2(it5ts); par-6(zu174)/+	1138/1311 (81%)	41/44 (93%)**
daf-7 par-2(it5ts); par-6(zu222)/+	550/654 (84%)	18/23 (78%)**
dpy-1 par-2(lw32) (20°C)	318/4459 (7%)	0/190
dpy-1 par-2(lw32); par-6(zu170)/+	639/826 (77%)	25/480 (5%)**
dpy-1 par-2(lw32); par-6(zu222)/+	3647/4798 (76%)	156/3647 (4%)
dpy-1 par-2(lw32); unc-101 par-6(zu222)/++	1233/1447 (85%)	72/1233 (6%)
dpy-1 par-2(lw32); hDf15/+	1760/3242 (54%)***	2/642 (<1%)
hDf15/hIn1	1334/1827 (73%)	

*Inferred genotype, see Materials and Methods for explanation.
**Only a subset of hatching progeny were scored for fertility.
*** Adjusted for the 25% lethality contributed by *hDf15* homozygotes.

The presence of detectable PAR-3 protein in *par-6* mutants was cell cycle dependent, with a higher percentage of pre-metaphase embryos showing staining than embryos in metaphase, anaphase, or telophase (see Fig. 6 legend). When peripheral staining was detectable, it was much fainter around the embryonic periphery than is observed in wild-type embryos. However, in two-cell and four-cell embryos, staining at the membranes between the blastomeres was quite pronounced.

Because *par-2(+)* activity is required to restrict PAR-3 protein to the anterior (Boyd et al., 1996), it was possible that the absence of PAR-3 protein at the periphery of *par-6* mutants could have been the indirect result of PAR-2 protein mislocalization. To test this hypothesis we stained *par-2; par-6* double mutants with PAR-3 antibody. We found that these embryos were indistiguishable from *par-6* embryos, with very little PAR-3 staining detectable at the cell periphery (data not shown).

par-6 mutations act similarly to *par-3* mutations in genetic tests

The immunolocalization results suggest that *par-6(+)* acts by mediating the peripheral localization of the PAR-3 protein. Genetic results are consistent with this model. We found that embryos from the double homozygote *par-3(it71)*; *par-6(zu170)* are indistinguishable in phenotype from *par-3(it71)* embryos. Furthermore, *par-6* mutations and a weak *par-3* mutation exhibit synergistic effects in double mutant combinations. As shown in Table 1, only 9% of double homozygote *par-6(zu170)*; *par-3(e2074)* embryos produce gut granules compared to 57% of *par-3(e2074)* embryos and 70% of *par-6(zu170)* embryos.

Mutations in *par-2* and *par-3* show opposite effects on the spindle orientations of the second cleavage. In *par-3* embryos, both blastomeres show longitudinal divisions, with the spindles oriented parallel to the long axis of the egg. In *par-2* embryos, both blastomeres divide transversely, with the spindles oriented perpendicular to the long axis (Fig. 3C). In *par-2; par-3* double mutants, AB and P1 both have longitudinal oriented spindles, indicating that *par-3* is epistatic to *par-2* (Cheng et al., 1995). If *par-6* acts by localizing PAR-3, then we expected that *par-6* mutations would also be epistatic to *par-2*. Indeed, we find that the AB and P1 spindles also are longitudinal in *par-2(lw32); par-6(zu222)* and *par-2(it5ts); par-6(zu222)* mutant embryos (Fig. 3D).

par-6 suppresses *par-2* alleles

In constructing the *par-2; par-6* double mutant we discovered that worms carrying one mutant copy of *par-6* bypass the need for a functional *par-2* gene. Hermaphrodites that are homozygous for the temperature-sensitive allele *par-2(it5ts)* produce only 8% hatching progeny at 25°C. Most of these hatching progeny become sterile adults lacking mature gametes. However, a homozygous *par-2* hermaphrodite that is heterozygous for any of the *par-6* mutations produces 81-85% hatching progeny, with 78-93% of these progeny becoming fertile adults (Table 2). Thus, the *par-6* mutations act as dominant suppressors of both the embryonic lethality and the adult sterility of *par-2(it5ts)*.

To test if this suppression was limited to the temperature-sensitive allele of *par-2*, we asked if *par-6* mutations could suppress other *par-2* mutations. *par-2(lw32)* allele is a nonsense mutation in the first third of the coding sequence (Levitan et al., 1994) and has a stronger phenotype than *it5*. We found that *par-2(lw32)* homozygotes that were heterozygous for either *par-6(zu170)* or *par-6(zu222)* produced 77% and 76% hatching progeny, respectively. We also observed some suppression in the adult sterility of the hatched progeny, with about 5% becoming fertile adults (Table 2).

To determine if this suppression results from loss-of-function at the *par-6* locus, we tested whether *par-2* worms heterozygous for a deficiency which deletes *par-6* would also be suppressed. We constructed a *par-2(lw32); hDf15/+* strain (see Materials and Methods) and scored the percentage of hatching embryos. 52% of the worms produced more viable embryos than ever observed for *par-2(lw32)* worms, with an average of 54% of embryos hatching (Table 2), indicating that *hDf15* also suppresses *par-2*. This suppression is less robust than suppression observed with the *par-6* alleles. This could indicate that suppression is sensitive to levels of *par-6* activity, could reflect differences in genetic background between the strains, or could mean that *hDf15* deletes other genes that play a role in the processes mediated by *par-6* and *par-2*.

DISCUSSION

We have described the characterization of *par-6*, a new gene necessary for the generation of polarity in early *C. elegans*

embryos. In *par-6* mutants, the first cleavage results in equal-sized blastomeres that undergo nearly synchronous divisions, have altered aster morphologies, and divide along the long axis. Late embryos arrest as amorphous masses of differentiated cells and the rare survivors of maternal effect lethality are agametic. This phenotype is very similar to that produced by mutations in a previously characterized gene, *par-3*. A probable explanation for this similarity is suggested by our genetic and immunolocalization results. We propose that *par-6(+)* acts through *par-3(+)* by localizing or maintaining the PAR-3 protein at the cell periphery.

The protein product of the *par-3* gene is localized to the anterior periphery of one-cell embryos (Etemad-Moghadam et al., 1995) and the products of the *par-1* and *par-2* genes are localized to the posterior periphery (Guo and Kemphues, 1995; Boyd et al., 1996). These patterns represent the earliest known molecular markers of anterior/posterior polarity in the *C. elegans* embryo, and understanding how these patterns are generated should provide insight into the first steps of embryogenesis. PAR-3 plays a role in determining the distributions of PAR-1 and PAR-2, because in *par-3* mutants these proteins are uniformly present at the periphery of the embryo (Etemad-Moghadam et al., 1995; Boyd et al., 1996).

In this paper, we provide evidence that the role of the *par-6* gene is to localize or maintain the PAR-3 protein at the cell periphery. Our genetic analysis indicates that *par-3* and *par-6* function in a common process. The mutant phenotypes are similar; strong *par-3* mutants are epistatic to *par-6* mutants, weak *par-3* mutants are enhanced by *par-6* mutants, and both *par-3* and *par-6* are epistatic to *par-2*. Our immunofluorescence results reveal at least one aspect of the relationship between the two genes: in the absence of *par-6(+)* activity, PAR-3 protein is greatly reduced or absent from the cell periphery. Western blots show that this is the result of failure to localize the protein rather than a consequence of reduction in synthesis or stability of the protein. The patchy distribution of PAR-3 in early stages of the cell cycle could reflect residual *par-6(+)* activity in the mutants or could mean that *par-6* is not required for initial localization of PAR-3. Furthermore, the failure of the patchy staining to be restricted to the anterior suggests that *par-6(+)* may play a role in the asymmetric distribtution of PAR-3.

An unexpected result from our double mutant analysis of *par-6* and *par-2* was the finding that reducing the amount of wild-type *par-6* can suppress *par-2* mutations. This is an example of bypass suppression since the suppression is not allele-specific with respect to *par-6* or *par-2* (Hartman and Roth, 1973). At least one other dominant bypass suppressor of *par-2* has been isolated (Cheng, 1991), demonstrating that the *par-6/+* background is not the only genetic background in which the requirement for the *par-2* gene product is reduced.

The suppression of *par-2* mutations can be explained in light of the proposed role for *par-6* in localizing or maintaining the localization of PAR-3. In wild-type one-cell embryos, the PAR-3 distribution is sharply defined, with high levels in the anterior and no detectable PAR-3 in the posterior. In *par-2* mutants, PAR-3 distribution becomes graded, remaining at high concentration in the anterior but now showing detectable protein in the posterior (Etemad-Moghadam et al., 1995). We propose that the abnormalities in *par-2* mutants result primarily from inappropriate posterior distribution of PAR-3. Reducing

the level or activity of PAR-3 in a *par-2* mutant (via removal of one copy of *par-6(+)*) might prevent PAR-3 function in the posterior, but permit PAR-3 to function in the anterior, and thus suppress embryonic lethality.

We found that PAR-1 and PAR-2 proteins fail to be restricted to the posterior in *par-6* mutants. This is also consistent with a role for *par-6(+)* in maintaining PAR-3 at the cell periphery, since in *par-3* mutants the asymmetrical distribution of PAR-1 and PAR-2 is also disrupted. PAR-1 is not involved in the anterior localization of PAR-3, since PAR-3 distribution in *par-1* mutants is normal (Etemad-Moghadam, 1995). However, PAR-2 is necessary for the restriction of PAR-3 to the anterior (Boyd et al., 1996), raising the possiblity that the presence of PAR-2 at the anterior of *par-6* mutant embryos is the basis for absence of peripheral PAR-3. This is ruled out by the finding that *par-2; par-6* double mutants also have very little PAR-3 at the cell periphery.

Mutants in *par-6* display aberrant SKN-1 localization. SKN-1 is a putative transcription factor that is necessary for the proper fate of the posterior blastomere, EMS (Bowerman et al., 1992) and is asymmetrically distributed at the two- and four-cell stages, such that the posterior blastomeres contain more SKN-1 than do anterior blastomeres (Bowerman et al., 1993). We show that in *par-6* embryos SKN-1 protein is sometimes localized to both the AB and P1 blastomeres at the two-cell stage and to all four blastomeres at the four-cell stage. Consistent with this distribution, some *par-6* embryos produce extra pharyngeal tissue, as is the case with *par-1* and *mex-1*, maternal effect lethal mutants that also mislocalize SKN-1 (Bowerman et al., 1993; Mello et al., 1992).

Germ-line specific P granules are abnormally localized in *par-6* embryos. The P-granule mislocalization in *par-6* mutants is consistent with a recent proposal that P granule localization in one-cell and two-cell embryos takes place by two mechanisms (Hird et al., 1996). The major mechanism is physical translocation of the granules to the posterior, a process mediated by cortical flow. A second mechanism is degradation or disaggregation of P granules that remain in the anterior. In wild-type embryos, P granules are always localized to the posterior by the time the male and female pronuclei meet. At this stage in *par-6* embryos, P granules are often still present in the cytoplasm of the anterior half of the embryo. However, by the time the zygote nucleus enters metaphase of the first cell cycle, few P granules remain in the anterior.

This phenotype may reflect an uncoupling of the proposed two-step process for P granule localization. We suggest that in *par-6* one-cell embryos, the mechanism for physical translocation of the granules is less effective than in wild-type embryos, causing many P granules to remain in the anterior, but the degradation mechanism remains functional such that by the end of the cell cycle most P granules still present in the anterior are degraded. It is also possible that the progressive restriction to the posterior in *par-6* embryos reflects a longer period during which migration of P granules can take place. In the P1 blastomere of *par-6* two-cell embryos, in contrast to one-cell embryos, P granules are evenly distributed to both daughters indicating a complete disruption of both mechanisms.

At the four-cell stage, P granules reappear in AB daughters of many *par-6* embryos, even though they are rarely observed in the AB cell at the two-cell stage. We suggest that the reap-

pearance of granules at the four-cell stage might reflect the deactivation of the normal system for eliminating mislocalized P granules. This could be an indirect consequence of the overall disruption of embryonic polarity. Early disappearance and subsequent reappearance of P granules also occurs in *par-1*, *par-3* and *par-4* embryos (Guo and Kemphues, 1995; K. J. Kemphues, unpublished results).

REFERENCES

Albertson, D. (1984). Formation of the first cleavage spindle in nematode embryos. *Dev. Biol.* **101**, 61-72.

Bowerman, B., Eaton, B. A. and Priess, J. R. (1992). *skn-1*, a maternally expressed gene required to specify the fate of ventral bastomeres in the early *C. elegans* embryo. *Cell* **68**, 1061-1075.

Bowerman, B., Draper, B. W., Mello, C. C. and Priess, J. R. (1993). The maternal gene *skn-1* encodes a protein that is distributed unequally in early *C. elegans* embryos. *Cell* **74**, 443-452.

Boyd, L., Guo, S., Levitan, D., Stinchcomb, D. T. and Kemphues, K. J. (1996). PAR-2 is asymmetrically distributed and promotes association of P granules and PAR-1 with the cortex in *C. elegans* embryos. *Development* (in press).

Brenner, S. (1974). The genetics of *Caenorhabditis elegans. Genetics* **77**, 71-94.

Cheng, N. (1991). Genetic and developmental analysis of *par-2*, a gene required for cytoplasmic localization and cleavage patterning in *Caenorhabditis elegans.* PhD thesis. Cornell University.

Cheng, N. N., Kirby, C. M. and Kemphues, K. J. (1995). Control of cleavage spindle orientation in *C. elegans*: the role of the genes *par-2* and *par-3*. *Genetics* **139**, 549-559.

Edgley, M., Baillie, D. L., Riddle, D. L. and Rose, A. M. (1995). Genetic balancers. In Caenorhabditis elegans: *Modern Biological Analysis of an Organism* (ed. H. G. Epstein and D. C. Shakes), pp. 147-184. San Diego: Academic Press.

Epstein, H. F., Miller, D. M. I., Gossett, L. A. and Hecht, R. M. (1982). Immunological studies of myosin isoforms in nematode embryos. In *Muscle Development: Molecular and Cellular Control* (ed. M. L. Pearson and H. F. Epstein), pp. 419-427. Cold Spring Harbor, New York: Cold Spring Harbor Laboratory Press.

Etemad-Moghadam, B., Guo, S. and Kemphues, K. J. (1995). Asymmetrically distributed PAR-3 protein contributes to cell polarity and spindle alignment in early *C. elegans* embryos. *Cell* **83**, 743-752.

Francis, G. R. and Waterston, R. H. (1985). Muscle organization in *Caenorhabditis elegans*: localization of proteins implicated in thin filament attachment and I-band organization. *J. Cell Biol.* **101**, 1532-1549.

Guo, S. and Kemphues, K. J. (1995). *par-1*, a gene required for establishing polarity in *C. elegans* embryos encodes a putative ser/thr kinase that is asymmetrically distributed. *Cell* **81**, 611-620.

Hartman, P. E. and Roth, J. R. (1973). Mechanisms of suppression. *Advan. Gen.* **17**, 1-105.

Hill, D. P. and Strome, S. (1990). Brief cytochalasin-induced disruption of microfilaments during a critical interval in 1-cell *C. elegans* embryos alters the partitioning of developmental instructions to the 2-cell embryo. *Development* **108**, 159-172.

Hird, S. N. and White, J. G. (1993). Cortical and cytoplasmic flow polarity in early embryonic cells of *Caenorhabditis elegans. J Cell Biol.* **121**, 1343-1355.

Hird, S. E., Paulsen, J. E. and Strome, S. (1996). Segregation of germ granules in living *Caenorhabditis elegans* embryos: cell-type-specific mechanisms for cytoplasmic localisation. *Development* **122**, 1303-1312.

Kemphues, K. J., Wolf, N., Wood, W. B. and Hirsh, D. (1986). Two loci required for cytoplasmic organization in early embryos of *Caenorhabditis elegans. Dev. Biol.* **113**, 449-460.

Hyman, A. A. and White, J. G. (1987). Determination of cell division axes in the early embryogenesis of *Caenorhabditis elegans. J. Cell Biol.* **105**, 2123-2135.

Kemphues, K. J., Kusch, M. and Wolf, N. (1988a). Maternal-effect lethal mutations on linkage group II of *C. elegans. Genetics* **120**, 977-986.

Kemphues, K. J., Priess, J. R., Morton, D. G. and Cheng, N. (1988b). Identification of genes required for cytoplasmic localization in early *C. elegans* embryos. *Cell* **52**, 311-320.

Kemphues, K. J. (1989). Caenorhabditis. In *Frontiers in Molecular Biology: Genes and Embryos* (ed. D. M. Glover and E. D. Hames), pp. London: IRL Press.

Kirby, C., Kusch, M. and Kemphues, K. (1990). Mutations in the *par* genes of *Caenorhabditis elegans* affect cytoplasmic reorganization during the first cell cycle. *Dev. Biol.* **142**, 203-215.

Laufer, J. S., Bazzicalupo, P. and Wood, W. B. (1980). Segregation of developmental potential in early embryos of *Caenorhabditis elegans. Cell* **19**, 569-577.

Lee, J., Jongeward, G. D. and Sternberg, P. W. (1994). Unc-101, a gene required from many aspects of *Caenorhabditis elegans* development and behavior, encodes a clathrin-associated protein. *Genes Dev.* **8**, 60-73.

Levitan, D. J., Boyd, L., Mello, C. C., Kemphues, K. J. and Stinchcomb, D. T. (1994). *par-2*, a gene required for blastomere asymmetry in *Caenorhabditis elegans*, encodes zinc finger and ATP binding motifs. *Proc. Nat. Acad. Sci. USA* **91**, 6108-6112.

Mello, C. C., Draper, B. W., Kraus, M., Weintraub, H. and Priess, J. R. (1992). The *pie-1* and *mex-1* genes and maternal control of blastomere identity in early *C. elegans* embryos. *Cell* **70**, 163-176.

Miller, D. M., Ortiz, I., Berliner, G. C. and Epstein, H. F. (1983). Differential localization of two myosins within nematode thick filaments. *Cell* **34**, 477-490.

Morton, D. G., Roos, J. M. and Kemphues, K. J. (1992). *par-4* a gene required for cytoplasmic localization and determination of specific cell types in *Caenorhabditis elegans* embryogenesis. *Genetics* **130**, 771-790.

Nigon, V., Guerrier, P. and Monin, H. (1960). L'Architecture polaire de l'oeuf et movements des constituants cellulaires au cour des premières étapes du développment chez quelque nématodes. *Bull. Biol. Fr. Belg.* **94**, 132-201.

Priess, J. R. (1994). Establishment of initial asymmetry in early Caenorhabditis elegans embryos. *Curr. Opin. Genet. Dev.* **4**, 563-568.

Rose, L. S., Lamb, M. L., Hird, S. N. and Kemphues, K. J. (1995). Pseudocleavage is dispensable for polarity and embryogenesis in *C. elegans* embryos. *Dev. Biol.* **168**, 479-489.

Strome, S. and Wood, W. B. (1982). Immunofluorescence visualization of germ-line-specific cytoplasmic granules in embryos, larvae, and adults of *Caenorhabditis elegans. Proc. Nat. Acad. Sci. USA* **79**, 1558-1562.

Strome, S. and Wood, W. B. (1983). Generation of asymmetry and segregation of germ-line granules in early *Caenorhabditis elegans* embryos. *Cell* **35**, 15-25.

Sulston, J., Schierenberg, E., White, J. and Thomson, N. (1983). The embryonic cell lineage of the nematode *Caenorhabditis elegans. Dev. Biol.* **100**, 67-119.

Waddle, J. A., Cooper, J. A. and Waterston, R. H. (1994). Transient localized accumulation of actin in *Caenorhabditis elegans* blastomeres with oriented asymmetric divisions. *Development* **120**, 2317-2328.

Wood, W. B., editor (1988). Embryology. In *The Nematode* Caenorhabditis elegans. Pp. 215-242. Cold Spring Harbor: Cold Spring Harbor Laboratory Press.

Wood, W. B. and Edgar, L. G. (1994). Patterning in the *C. elegans* embryo. *Trends Genet.* **10**, 49-54.